

Age Hardening and Quench Sensitivity of Aluminium Alloys

Introduction

Previous versions of JMatPro®, prior to the Ver. 11, have contained models for both strength and precipitation kinetics. However, they have not been combined to produce Age Hardening curves or an explicit consideration of Quench Sensitivity. This has now been achieved in Ver. 11, where the strength and kinetic models are combined, hereafter referred as the integrated model, to provide new capabilities to account for both of these important phenomena.

The kinetic models in Ver. 10, with the exception of the transition from GP zones to secondary metastable hardening phases, only considered the formation of each phase individually from the supersaturated Al matrix. However, the strength model utilises strengthening from the metastable phases formed at the heat treatment temperature. As such multiple phases may be formed and we have followed the Shercliff and Ashby concept [1] that these phases are formed simultaneously during heat treatment and, in the present case, at a rate controlled by the dominant hardening phase(s). It is recognized that the transformation in reality will be more complex, but trying to explicitly model the formation of multiple phases is extremely convoluted and possibly outside the scope of current kinetic models for application to all types of aluminium alloys. The final result with the simplified model does, though, appear to give rather good and useful capability for modelling of strengthening during heat treatment, as demonstrated later in this report.

GP hardening has also been included in the model, using a shear strengthening model similar to that of Shercliff and Ashby [1,2], so that natural ageing can now be considered as well as the transformation of GP zones to metastable hardening phases such as S' and eta' for alloys from the 2000 and 7000 series during T5 and T6 tempering. Otherwise details for the models for precipitation hardening and precipitation kinetics have been provided in previous publications [3,4,5]. This note is focused on demonstrating the performance of this integrated model against experimental data on heat treatment time, age hardening curve and quench sensitivity of commercial alloys. As the kinetic models have been further improved during the assessment of the integrated model, the resulting changes in TTT/CCT diagrams and isothermal ageing kinetics are discussed in comparison with the calculations of Ver. 10. The advantages and limitations of this integrated approach are discussed as well.

Model Assessment on Heat Treatment Time of Commercial Alloys

Generally speaking, many hardening curves reported in the literature have significant issues in terms of validating models that would be applicable to commercial alloys. As JMatPro® is a tool designed for commercial alloys, it is important to validate the model in this context. To that end, model parameters were evaluated so they reach peak strength within the standard heat treatment time at the ageing temperature for commercial alloys. This is a rational assumption as the time of artificial ageing is usually chosen to achieve the peak hardness without significant overaging unless desired. As such, the peak position of an alloy should be no longer than its commercial heat treatment time at the given ageing temperature. Fig. 1 shows a comparison of time to reach 99% calculated peak strength vs heat treatment times (t_c) of a wide range of commercial alloys. As can be seen most of the calculated peak times fall in the range of $t_c/2$ to t_c , which appears very reasonable.

Model Assessment on Age Hardening Curves

While there are a reasonable number of age hardening curves reported in the literature, many of these curves do not provide results consistent with the standard heat treatment schedules operated in practice for commercial alloys. For example, an often-quoted work on alloy 6061, e.g. by Shercliff and Ashby [1,2], is

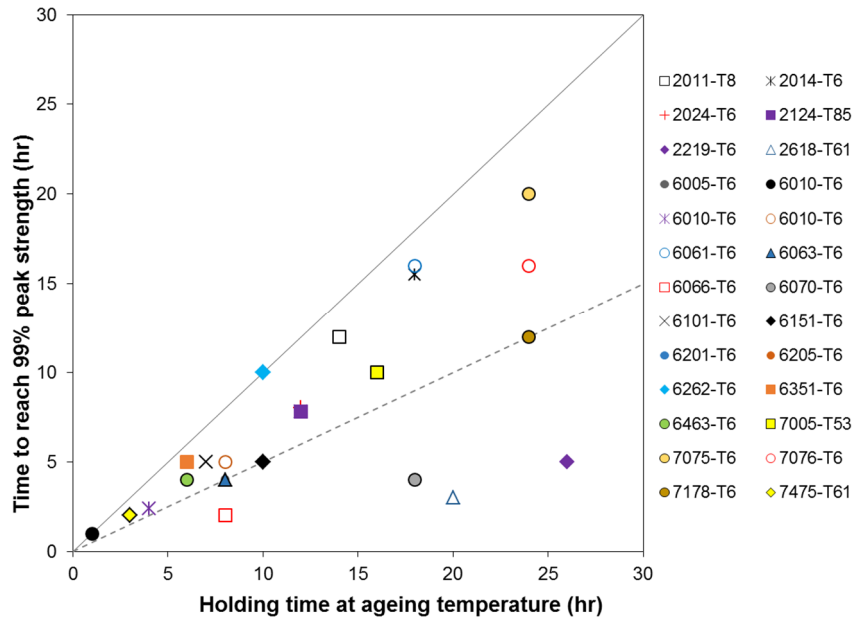


Fig. 1: Calculated peak positions vs heat treatment times of commercial alloys.

from Anderson [6] and Fig. 2 shows its hardening behaviour during ageing at 163°C (the T6 temperature for 6061 is 160°C). The dotted lines are the T6 treatment time and yield strength of this alloy in practice, i.e. 18 hours and 275 MPa [7]. It is clear that peak strength would not take place in this time and is only reached after 90 hours. The calculated peak position and strength, on the other hand, coincides very well with this schedule. It should be noted that the experimental as-quenched hardness value is substantially higher than would be expected for the unhardened, quenched state. Therefore some hardening has already occurred and the reasons for that will be discussed later.

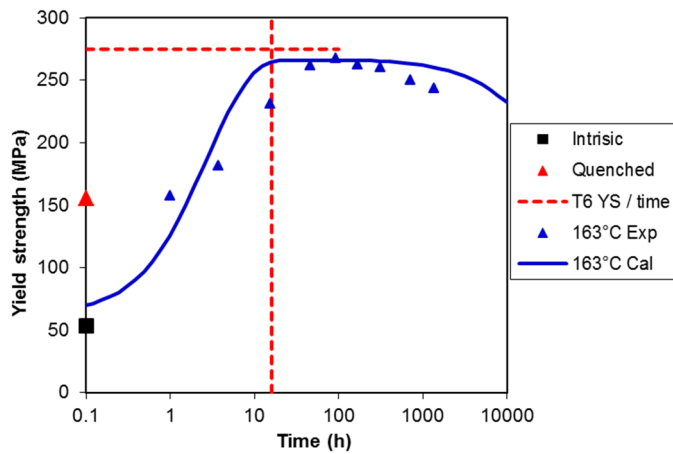


Fig. 2: Age hardening of alloy 6061, with experimental hardening curve from Anderson [6] and T6 strength/time from ASM Handbook [7].

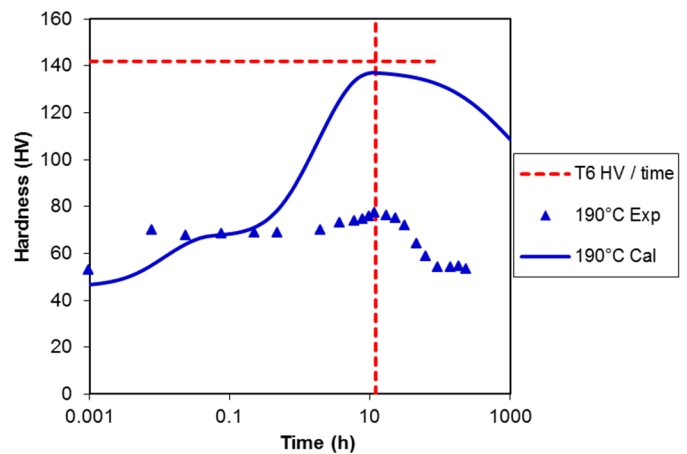


Fig. 3: Age hardening of alloy 2024, with experimental hardening curve from Shih et al. [8] and T6 hardness/time from ASM Handbook [7].

Generally speaking, the values of peak strength from various sources do not differ much for the same alloy, but the same cannot be said for peak hardness in many reported ageing curves. For example, Fig. 3 shows the age hardening curve of alloy 2024 at T6 temperature 190°C [8]. The peak hardness is about HV 80 here, which is much lower than the reported T6 hardness of HV 142 in the ASM handbook for the same alloy [7]. Another example is for alloy Al-4wt%Cu. Its peak hardness, firstly reported by Hardy [9] and then quoted in the work of Shercliff and Ashby [1], is shown to be around HV 90, whereas a value of over HV 130 was reported by Lumley et al. [10].

The current model allows natural ageing to be considered and Fig. 4 shows natural ageing curves for alloys 2024, 6061 and 7075. For both 2024 and 7075 the calculated strengths show an initial quite rapid increase in strength consistent with observation, which is associated with the formation of GP zones. There is then a plateau before a secondary hardening occurs as the GP zones transform to S' and eta' prime respectively. For 2024, secondary hardening only occurs after the experimental measurements stopped and is fully consistent with observed behaviour. For 7075, the secondary hardening appears slightly earlier, providing further strengthening within the time of the experiments, which is consistent with experiment. However, it exhibits a plateau where the GP zone retains its stability before transformation to eta' occurs rather than the more general rise shown in Ref. 7.

For 6061, the calculated hardening is delayed in comparison to experiment and reaches a value substantially higher than observed in the later stages. This may be due to the formation of relatively stable clusters as postulated in a number of publications [11,12,13], which may both provide both a hardening effect and delay the onset of formation of the metastable Mg_xSi_y phases. Such clusters are not taken into account in the present modelling. Cluster may also form at higher temperatures as a precursor to the metastable Mg_xSi_y phases but in this case would not appear to noticeably delay their formation.

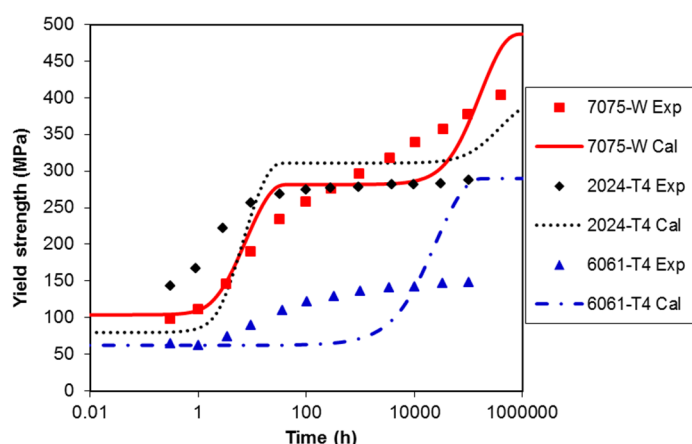
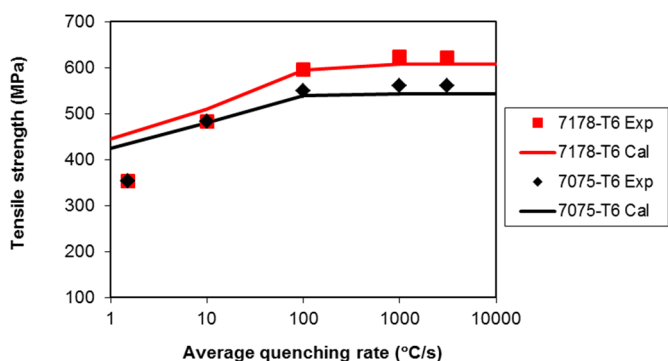


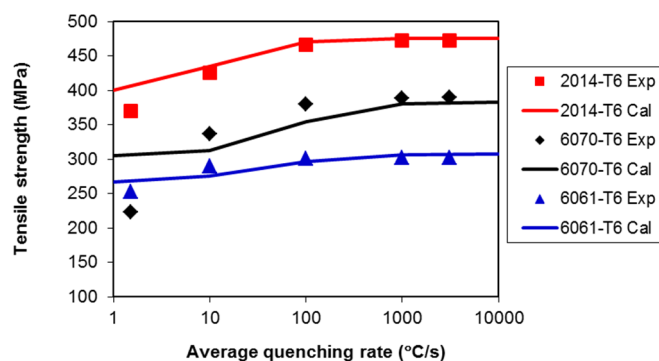
Fig. 4: Natural age hardening curves of alloys 2024, 6061 and 7075, with experimental data from Ref. 7.

Model Assessment on Quench Sensitivity

Experimental data on quench sensitivity usually appear in the form of yield strength, tensile strength or hardness as a function of quenching rates. The data used in the current assessment are taken from Refs. 7 and 14, covering 2000, 5000, 6000, 7000 and 8000 series, Figs. 5-7. Fig. 5 shows the tensile strength of alloys 2014, 6061, 6070, 7075 and 7178 in T6-treated conditions as a function of quench rates. In agreement with the observed behaviour, it can be clearly seen that the quench rate of these alloys should not go below 100°C/s to avoid significant loss of strength due to cooling.



(a) T6 of 7178 and 7075



(b) T6 of 2014, 6070 and 6061

Fig. 5: Quench sensitivity of various Al-alloys as a function of average quench rates: tensile strength of alloys in T6-treated condition.

Fig. 6(a) shows the yield strength of alloys 6061 and 7050 in T6-treated conditions as a function of quench rates, whereas Fig. 6(b) is for yield and tensile strength of alloy 2024 in T4 condition. A similar trend is observed with strengths falling as cooling rates fall below 100°C.

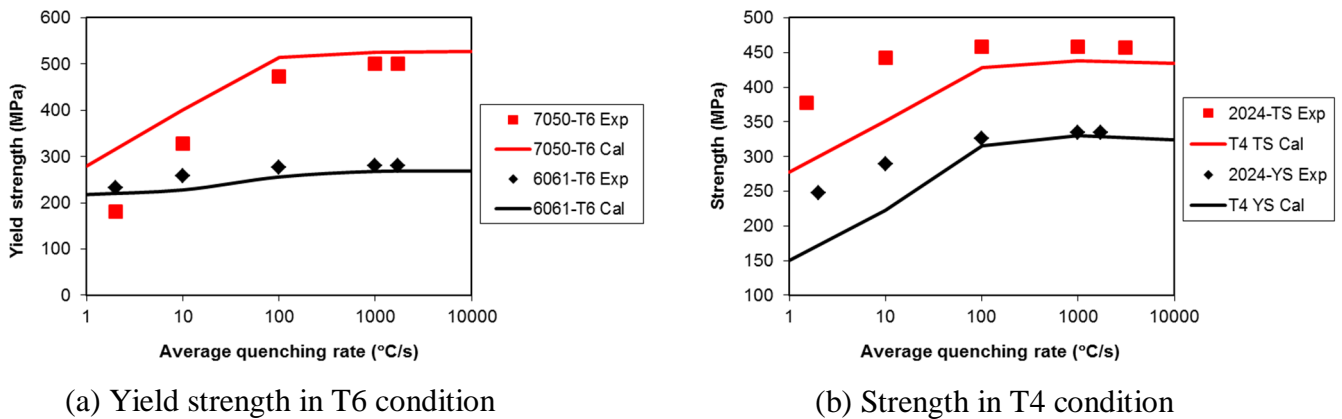


Fig. 6: Quench sensitivity of various Al-alloys as a function of average quench rates: (a) yield strength of alloys in T6-treated condition, (b) yield and tensile strength in T4-treated condition.

Another way of showing the quench sensitivity of an alloy is to calculate the ratio of strength to the water quenched (WQ) yield strength, which is usually sufficient to prevent transformation on cooling, and display the results as a function of quench rate. Fig. 7 shows results for two Al-Li alloys (2090 and 8090, both solution-treated for 1 hour at 520°C) and two Zn-Mg-Cu Al-alloys (7475 and 7150, both solution-treated for 40 minutes at 480°C) as a function of average quench rates.

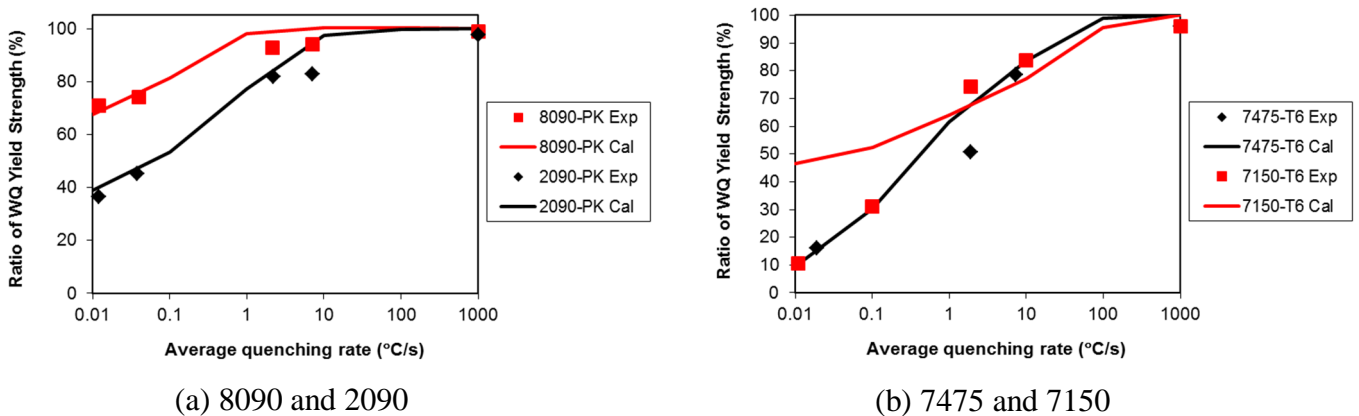
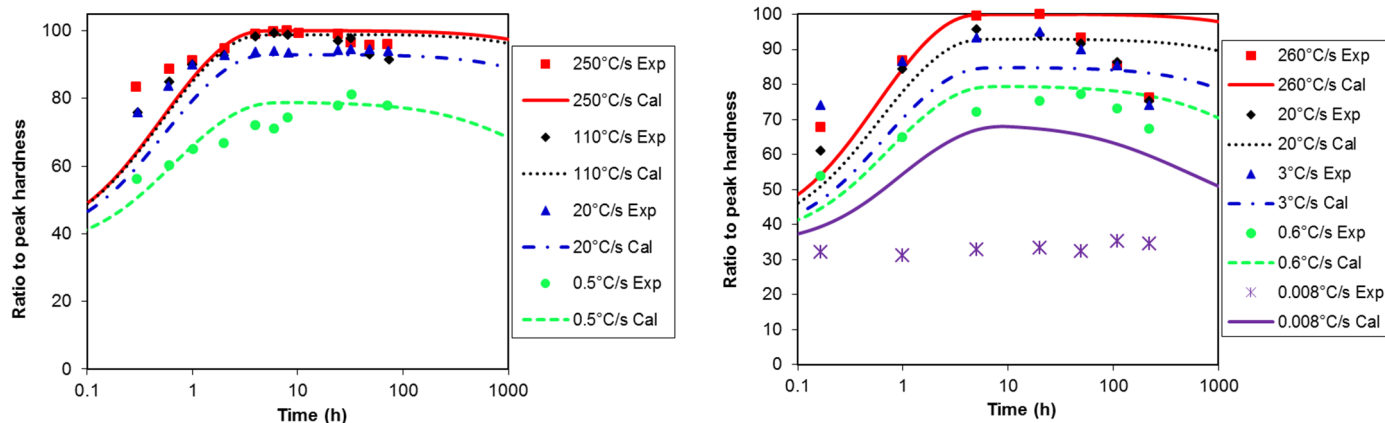


Fig. 7: Quench sensitivity of (a) Al-Li alloys and (b) Zn-Mg-Cu alloys as a function of average quench rates: ratio to WQ yield strength of alloys in T6-treated condition.

One of the advantages of being able to calculate quench sensitivity is that strength across a large casting can be calculated at various position in the casting itself. For example, the age hardening behaviour of alloy 356 at different quench rates was studied by Zhang et al. [15] and Fracasso [16]. Although the alloy is a casting grade, all samples in these two studies were solution treated before quenching, followed by ageing at 170°C. In the study of Zhang et al., the cooling rates were estimated as 0.5, 20, 110 and 250°C/s, respectively. A comparison between calculations and experimental data is given in Fig. 8(a), showing that strength loss becomes noticeable at cooling rate 20°C/s, and is significant when cooling rate is 0.5°C/s. In the work of Fracasso, the cooling rates cover the range of 0.008 – 260°C/s. Fig. 8(b) shows a comparison between calculations and experimental data of this study. Again, the strength drop becomes noticeable at cooling rate 20°C/s, and is more significant at slower cooling rates. At early stage of the curves up to 1 hour, the calculation deviates from the experimental data, but the peak time and peak hardness are generally in good agreement apart from the one at 0.008°C/s.



(a) Ratio to peak hardness – Zhang et al.

(b) Ratio to peak hardness – Fracasso

Fig. 8: Age hardening curves of alloy Al-356 at different quench rates – ratio to peak hardness. The experimental data were from Zhang et al. [15] in (a) and Fracasso [16] in (b).

Current Kinetic Modelling Compared to Ver. 10

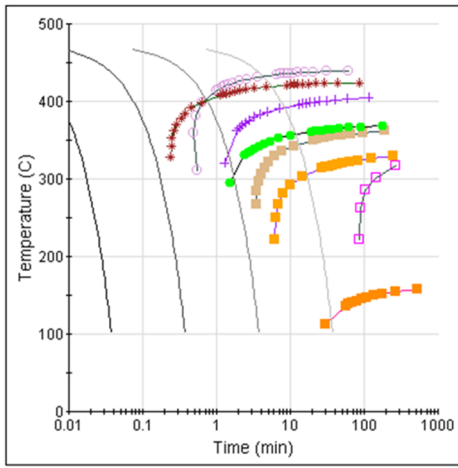
As the integrated model can now directly calculate quench sensitivity it became apparent that the kinetic parameters assessed for the stable phases in Ver.10 produced little loss in strength at slower cooling rates such as 10°C/s , in contradiction to observation. It also became clear that the critical volume fraction of precipitate forming during cooling should be nearer 0.5% rather than the value of 0.1% used in Ver.10. The kinetic parameters of the high temperature stable phases have therefore been re-assessed by accelerating their formation. A comparison of the TTT/CCT diagrams for 0.5% phase calculated in Ver. 10 and from the current assessment is given in Figs. 9 and 10, respectively. Generally speaking, the formation kinetics for most phases, with the exception of GP, are faster in the current assessment. On the other hand, the kinetics of transformation when GP zones are involved remains rather similar to that produced in Ver. 10 and a comparison of isothermal kinetics for 7075 at the T6 temperature of 120°C is shown in Fig. 11. The main difference is that the formation of η' is slightly accelerated so that peak hardening is achieved in the T6 heat treatment time of 24 hours [14].

Discussions - Early Stages of Heat treatment

One of the features observed in the early stages of experimental ageing curves is that both the initial strength prior to ageing and the strength in the early stages of heat treatment can be significantly higher than modelled. That may be simply due to the fact that current model does not take into account any time/temperature history an alloy may be subjected to prior to ageing. Instead, the current model assumes that an alloy is quenched to the ageing temperature and subsequently undergoes isothermal heat treatment.

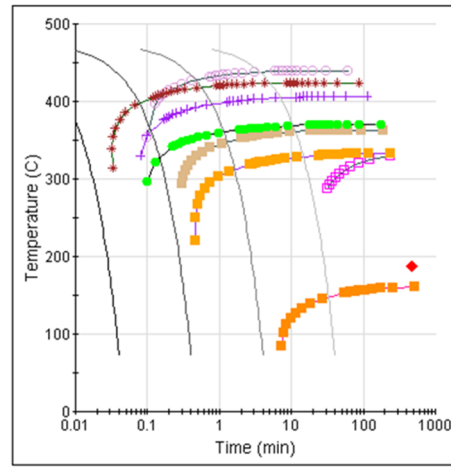
In usual practice, an alloy would be quenched to room temperature and may be held there for some time before undergoing a T5 or T6 heat treatment. For many types alloy, e.g. Steels, Ni-based alloys, etc., there is no transformation prior to ageing and such an assumption works well. But Al alloys of most types may undergo natural ageing during this time. Furthermore, kinetics in the heating range can be quite rapid with the potential for further hardening taking place during heating and thermal equilibration at the ageing temperature, see for example Fig. 3.

However, while such potential hardening is not currently taken into account, it is noticeable that after a quite short time, usually within an hour, the calculated curve starts to match experiment much more closely (Figs. 2 and 8). As such, for most of the commercial heat treatment schedule JMatPro should provide sound results for strength vs. time. It is intended to provide a much more complete time/temperature history for heat treatment in a future version of JMatPro that hopefully will address the initial stages of hardening more closely.



Quench temperature: 475.0 C

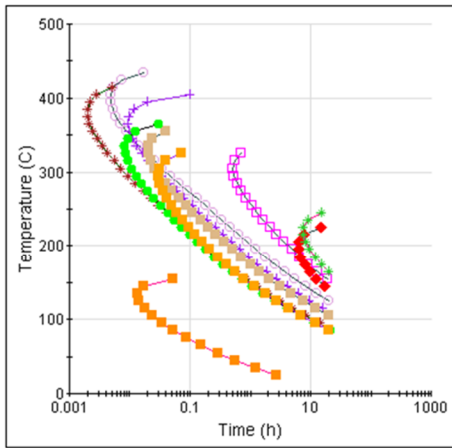
(a) CCT – Ver. 10



Quench temperature: 475.0 C

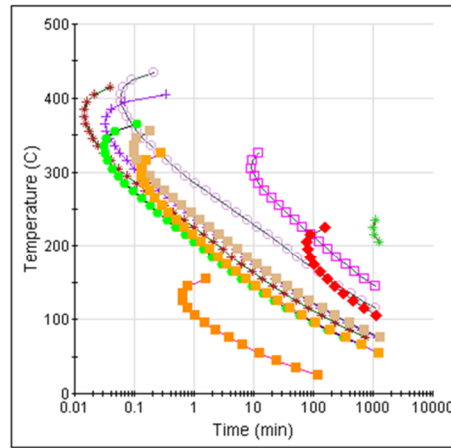
(b) CCT – current assessment

Fig. 9: Comparison of the CCT diagrams for alloy 7075, (a) calculated in Ver. 10, and (b) from the current assessment.



Quench temperature: 475.0 C
Cooling rate from quench temperature (C/s): 300.0

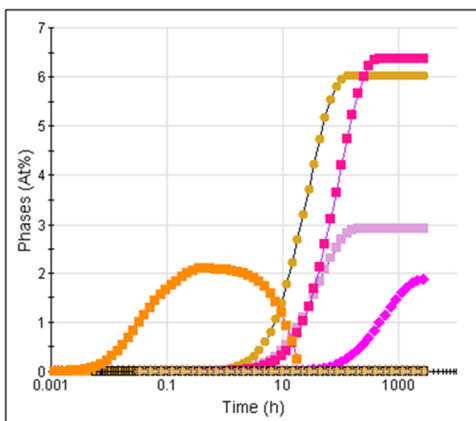
(a) TTT – Ver. 10



Quench temperature: 475.0 C
Cooling rate from quench temperature (C/s): 300.0

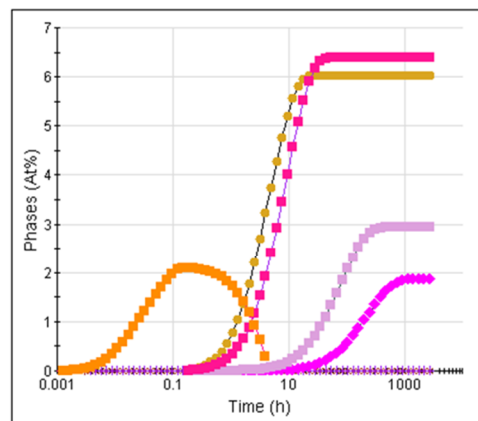
(b) TTT – current assessment

Fig. 10: Comparison of the TTT diagrams for alloy 7075, (a) calculated in Ver. 10, and (b) from the current assessment.



Quench temperature (C): 475.0
Holding temperature (C): 120.0
Cooling rate from quench temperature (C/s): 300.0

(a) Isothermal – Ver. 10



Quench temperature (C): 475.0
Holding temperature (C): 120.0
Cooling rate from quench temperature (C/s): 300.0

(b) Isothermal – current assessment

Fig. 11: Comparison of the isothermal kinetics for alloy 7075, (a) calculated in Ver. 10, and (b) from the current assessment.

Concluding Remarks

The integrated kinetics-strength model has been validated against experimental data over a wide range of commercial alloys. It proves to be a very useful tool to study the heat treatment of Al-alloys as well as their quench sensitivity and covers the following aspects.

1. It allows the formation of stable precipitates to come out during cooling. The strengthening contribution of these phases are considered in the calculation, but is invariably very low in comparison to the strengthening phases.
2. As a result of the precipitate formation during cooling, the amount of solutes in the matrix is changed, affecting its precipitation hardening potential during ageing treatment, i.e. the so-called quench sensitivity.
3. Potential strengthening (metastable) phases are allowed to precipitate out during ageing, generating the age hardening response curve.

References

-
- 1 H.R. Shercliff and M.F. Ashby, A process model for age hardening of aluminium alloys – I. The model, *Acta Metall. Mater.* 38:10 (1990), 1789-1802.
 - 2 H.R. Shercliff and M.F. Ashby, A process model for age hardening of aluminium alloys – II. Applications of the model, *Acta Metall. Mater.* 38:10 (1990), 1803-1812.
 - 3 Z. Guo, N. Saunders, A.P. Miodownik and J.P. Schillé, *Hot deformation of aluminium alloys*, Sente Software Ltd., 2016.
 - 4 Z. Guo, N. Saunders and J.P. Schillé, *Age hardening of aluminium alloys*, Sente Software Ltd., 2018.
 - 5 Z. Guo and N. Saunders, Modelling quench sensitivity of aluminium alloys, in *Proceedings of The International Conference on Aluminum Alloys (ICAA16)*, 17-21 June 2018, Montreal, Canada.
 - 6 W.A. Anderson, Precipitation hardening of aluminum base Alloy, in *Precipitation from Solid Solution*, American Society for Metal, Metal Park, Ohio (1959), 150-207.
 - 7 J.R. Davis, Ed., *Aluminum and Aluminum Alloys*, ASM Specialty Handbook, ASM International, 1993.
 - 8 H.C. Shih, N.J. Ho and J.C. Huang, Precipitation behaviors in Al-Cu-Mg and 2024 aluminum alloys, *Metall. Mater. Trans.*, 27A (1996), 2479-2494.
 - 9 H.K. Hardy, The ageing characteristics of binary aluminium-copper alloys, *J. Inst. Metals* 79 (1951), 321-369.
 - 10 R.N. Lumley, I.J. Polmear and A.J. Morton, Interrupted Aging and Secondary Precipitation in Aluminium alloys, *Materials Science and Technology*, 19:11 (2003), 1483-1490.
 - 11 A. Serizawa, S. Hirosawa and T. Sato, Three-dimensional atom probe characterisation of nanoclusters responsible for multistep aging behavior of an Al-Mg-Si alloy, *Metall. Mater. Trans* 39A (2008), 243-251.
 - 12 K. Matsuda, T. Kawabata, Y. Uetani, T. Sato, A. Kamio and S. Ikeno, HRTEM observation of G.P. zones and metastable phase in Al-Mg-Si alloys, *Materials Science Forum*, 331-337 (2000), 989-994.
 - 13 A.K. Gupta and D.J. Lloyd, Study of precipitation kinetics in a super purity Al-0.8 Pct Mg-0.9 Pct Si alloy using differential scanning calorimetry, *Metall. Mater. Trans.* 13A (1999), 879-890.
 - 14 H. Chandler, Ed., *Heat Treating Guide – Practices and Procedures for Nonferrous Alloys*, ASM International, 1996.
 - 15 D.L. Zhang and L. Zhang, The Quench Sensitivity of Cast Al-7wt%Si-0.4wt%Mg Alloy, *Metall. Mater. Trans.* 27A (1996), 3983-3991.
 - 16 F. Fracasso, Influence of quench rate on the hardness obtained after artificial ageing of an Al-Si-Mg alloy, PhD Thesis, Jönköping Institute of Technology, 2010.